Live Attenuated Measles Virus Vaccine Expressing *Helicobacter pylori* Heat Shock Protein A

Ianko D. Iankov,[1,2] Cheyne Kurokawa,[1] Kimberly Viker,[1] Steven I. Robinson,[1,2] Arun Ammayappan,[1] Eleni Panagioti,[1] Mark J. Federspiel,[1] and Evanthia Galanis[1,2]

[1]Department of Molecular Medicine, Mayo Clinic, 200 First Street SW, Rochester, MN 55905, USA; [2]Division of Medical Oncology, Mayo Clinic, 200 First Street SW, Rochester, MN 55905, USA

Measles virus (MV) Edmonston derivative strains are attractive vector platforms in vaccine development and oncolytic virotherapy. *Helicobacter pylori* heat shock protein A (HspA) is a bacterial heat shock chaperone with essential function as a Ni-ion scavenging protein. We generated and characterized the immunogenicity of an attenuated MV strain encoding the HspA transgene (MV-HspA). MV-HspA showed faster replication within 48 h of infection with >10-fold higher titers and faster accumulation of the MV proteins. It also demonstrated a superior tumor-killing effect *in vitro* against a variety of human solid tumor cell lines, including sarcoma, ovarian and breast cancer. Two intraperitoneal (i.p.) doses of 10^6 50% tissue culture infectious dose ($TCID_{50}$) MV-HspA significantly improved survival in an ovarian cancer xenograft model: 63.5 days versus 27 days for the control group. The HspA transgene induced a humoral immune response in measles-permissive Ifnarko-CD46Ge transgenic mice. Eight of nine animals developed a long-term anti-HspA antibody response with titers of 1:400 to 1:12,800 without any negative impact on development of protective anti-MV immune memory. MV-HspA triggered an immunogenic cytopathic effect as measured by an HMGB1 assay. The absence of significant elevation of PD-L1 expression indicated that vector-encoded HspA could act as an immunomodulator on the immune check point axis. These data demonstrate that MV-HspA is a potent oncolytic agent and vaccine candidate for clinical translation in cancer treatment and immunoprophylaxis against *H. pylori*.

INTRODUCTION

Measles virus (MV) belongs to the Paramyxoviridae family. It has a negative strand RNA genome encoding six structural and two nonstructural proteins. MV has a lipoprotein envelope with two surface glycoproteins, that is, hemagglutinin (H) and fusion protein (F), responsible for virus attachment and entry into the host cells.[1] MV has exclusive human and high primate tropism, causing the most contagious infectious disease with more than 1.5 million estimated cases and >140,000 fatalities in 2018.[2] An immunoprophy-lactic strategy based on the live attenuated MV Edmonston vaccine strain has significantly reduced the morbidity and mortality rate caused by wild-type virus. The MV vaccine has an excellent safety track record with millions of doses administered worldwide annually. In addition, MV vaccine strain derivatives are promising oncolytic anti-cancer agents that can selectively infect and destroy transformed cells of solid tumor or hematologic malignancy origin.[3] Clinical trials for treatment of patients with ovarian cancer, brain tumor, and multiple myeloma are ongoing.[4] Reverse genetic engineering and rescue of recombinant MV strains has made possible insertion of different foreign antigens, reporters, and therapeutic genes into the MV genome.[5–7] In our previous studies we successfully cloned and characterized recombinant MV vaccine strains encoding *H. pylori* neutrophil-activating protein (NAP) constructs.[8,9]

H. pylori is a gastrointestinal tract pathogen associated with acute and chronic gastritis, peptic ulcer, gastric cancer, and gastric mucosa-associated lymphoid tissue (MALT) lymphomas.[10–12] Initial infection usually occurs early in childhood, with the chronic carrier rate exceeding more than 80%–90% of the adult population in developing countries.[13] The current therapeutic approach is based on triple and quadruple combinations of antibiotics, proton pump inhibitors, and bismuth compounds.[14] However, the high rate of infection recurrence and the increasing reports of antibiotic-resistant strains are the major hurdles for *Helicobacter* eradication strategy.[5] These factors and the expected population benefits and cost-effectiveness urge the development of successful vaccine approaches for the prevention and control of *H. pylori* infection.[15,16] We have previously shown that live MV vaccine strains encoding the secretory form of NAP (s-NAP) antigen induced a robust anti-NAP response.[8,9] The MV-s-NAP strain significantly improved anti-tumor activity against metastatic breast cancer,[17] and a phase I clinical
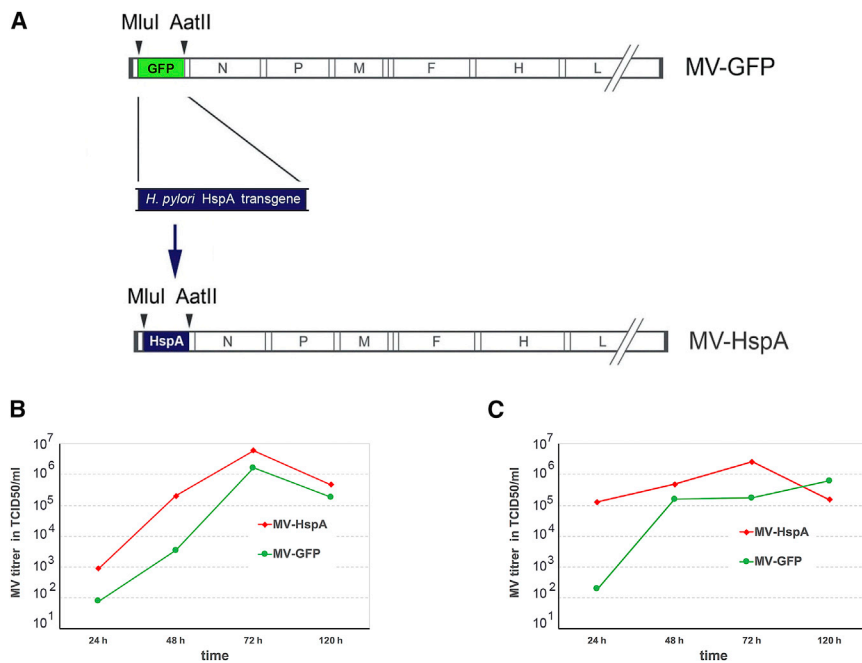
A

B

C

Figure 1. Schematic Representation and Growth Kinetics of Recombinant MV-HspA Strain

(A) HspA was cloned into the full-length MV plasmid DNA by replacing GFP at an additional transcriptional unit before the N gene using MluI and AatII endonuclease enzymatic sites. (B and C) Growth kinetics of MV-HspA in Vero cells compared to the control MV-GFP released in supernatant (B) and cell-associated virus (C). Supernatants were titrated directly on Vero cells. Cell-associated virus titers were determined by collecting the infected cells in Opti-MEM and subsequent Vero cell titration.

trial in breast cancer patients has recently received US Food and Drug Administration (FDA) approval.

H. pylori heat shock protein A (HspA) is one of the key virulence factors and protective antigens against *H. pylori* together with CagA, VacA, NAP, and urease.[18,19] HspA is a small 118-aa residue protein and a homolog of bacterial GroES chaperones with a unique Ni^{2+}-chelating domain at the C terminus.[20,21] HspA interacts with Ni^{2+} and subsequently releases the ions as part of the essential process for *H. pylori* Ni^{2+} homeostasis. Ni^{2+} is an important co-factor required for maturation and enzymatic activity of *H. pylori* urease, another key virulence factor for pathogen survival in an aggressive low pH microenvironment at the gastric mucosal surface. HspA has an extremely high affinity for Bi^{3+} ions, which block the protein function, and is the main mechanism of bismuth compound treatment effects.[22] With its key role in bacteria survival at the gastroduodenal mucosal surfaces, HspA represents one of the main targeted antigens in vaccine development against *H. pylori*. Previous studies using purified recombinant HspA as part of a multicomponent protein vaccine demonstrated the protective efficacy in a Mongolian gerbil model.[23] Protection depended on the adjuvant type, correlated strongly with antibody titers, and was associated with the predominant T helper (Th)2-type cellular immune response. The use of a two-component subunit vaccine using HspA and γ-glutamyl transpeptidase protected mice against *H. pylori* colonization by inducing strong systemic and local humoral immune response.[24] In another study, a fusion tricomponent recombinant antigen of urease, HspA, and *H. pylori* adhesion A (HpaA) proteins, but not the single antigens alone, induced strong antibody-mediated protection against *H. pylori* infection in BALB/c mice.[25] These data demonstrated the major role of HspA as a key virulence factor and antigen in the infection pathogenesis and

development of the protective immune response. However, all of the previous studies were focused on evaluation of immunogenicity of the formulated purified antigen but not of vector-encoded HspA.

In this study, we present the construction and characterization of recombinant MV Edmonston vaccine strain engineered to express *H. pylori* HspA antigen. The novel MV-HspA strain demonstrated enhanced anti-tumor activity as an oncolytic agent and strong immunogenic potential. In addition to the anti-tumor properties discussed herein, this strain could be used as the backbone for the development of a combined vaccination approach against measles and *Helicobacter* infection.

RESULTS

Rescue and Growth Characteristics of Recombinant MV-HspA

The PCR product of fragment *H. pylori* HspA from strain 26695 was cloned in TA-cloning vector and the correct DNA sequence was verified. The MluI/AatII digested fragment was subsequently inserted in the full-length p(+)MV-enhanced green fluorescent protein (EGFP) infectious clone plasmid of attenuated MV Edmonston strain upstream of the N protein gene (Figure 1A). The insert followed the "hexameric rule" required for successful rescue and replication of recombinant MV.[26] Full-length p(+)MV-HspA integrity and the HspA transgene were confirmed by analytical restriction enzyme digestion and DNA sequencing. MV-HspA was rescued on a 293-3-46 cell system using co-transfection of the MV plasmid with N and L protein-encoding plasmids. MV-HspA was amplified on the Vero cell line to passages 2 and 3, and titers were determined on Vero cells. Control MV strains were amplified in the same way, and corresponding passages 2 and 3 were used in all subsequent *in vitro* and *in vivo* experiments. Growth kinetics experiments with MV infection of Vero cells at a multiplicity of infection (MOI) of 1 demonstrated a different pattern of replication between MV-HspA and other MV strains. MV-HspA did not follow the growth characteristics of the MV strain expressing green fluorescent protein (MV-GFP) and replicated faster in Vero cells with rapid accumulation within the first 24–48 h of infection both as cell-associated and released in the supernatant infectious virus particles (Figures 1B and 1C). The titer for supernatant
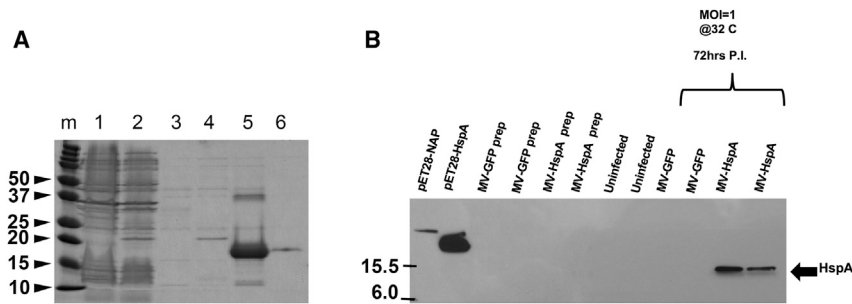
Figure 2. SDS-PAGE Analysis of Purified HspA and Western Immunoblotting for Detection of HspA Expression by MV-HspA-Infected Cells

(A) Fractions 1 and 2 (lanes 5 and 6) correspond to Ni-NTA column-eluted 6-His-tagged HspA. The protein was produced in *E. coli* BL21 Star (D3) cells. An insoluble crude fraction from pET-28a-transfected bacteria and column wash were loaded on lanes 1 and 3. Crude extract and an Ni-NTA-purified fraction from irrelevant *H. pylori* NAP 6-His-tagged recombinant protein are shown in lanes 2 and 4, respectively. MW protein standards (lane m) on the left show the HspA band between the 15- and 20-kDa markers corresponding to the predicted ~16.5-kDa MW size of the 6-His-tagged HspA protein. (B) Immunoblotting using a polyclonal mouse antibody demonstrated HspA protein accumulation following 72-h MV-HspA infection of Vero cells at 32°C. Presented results are from duplicate samples with MV-GFP used as the control strain. Ni-NTA-purified recombinant HspA was used as positive control.

MV-HspA was >10-fold and for the cell-associated viruses was >100-fold higher than that for the MV-GFP control at the 24-h time point. At the peak of amplification both MV-GFP and MV-HspA reached similar titers. Passage 3 of parallel grown MV-GFP and MV-HspA had similar titers of 4.67×10^7 and 5.53×10^7 50% tissue-culture infectious dose ($TCID_{50}$)/mL, respectively. These results indicated that insertion of the HspA transgene did not interfere negatively but rather improved MV replication at the early steps of infection.

Purification of Recombinant HspA and Detection of HspA Expression by MV-HspA-Infected Cells

HspA was cloned into the pET28a bacterial expression vector using BamHI/NotI sites with a 6-histidine (His)-tagged peptide sequence at the N terminus. His-tagged HspA was purified from transformed *E. coli* BL21 Star (DE3) bacteria using the Ni-nitrilotriacetic acid (NTA) fast kit under denaturing conditions. Protein concentration was measured by absorbance at 280 nm. The eluted fractions were analyzed by sodium dodecyl sulfate-polyacrylamide gel electrophoresis (SDS-PAGE) on 15% Criterion gel under reducing conditions (Figure 2A). The HspA preparation showed high-purity grade with correspondence to the theoretically expected molecular weight (MW) band at ~16.5 kDa of the recombinant protein. The HspA transgene is expressed at a high level by infected cells, as confirmed by immunoblotting (Figure 2B). Vero cells were infected at an MOI of 1, and cell lysates were analyzed at 72 h of incubation at 32°C by immunoblotting using the polyclonal mouse anti-HspA serum antibody. Purified *H. pylori* NAP from pET-28-NAP plasmid-transformed bacteria was used as a control. Recombinant HspA encoded by pET28-HspA plasmid appeared at a higher MW because of the longer 6-His-tagged peptide at the N terminus expressed, while MV-HspA expressed the full-length natural HspA sequence.

MV-HspA Showed a Significantly Improved Anti-tumor Effect as Compared to Control MV Strains against Different Solid Tumor Types

In one-step viral growth curves (MOI of 1 at 32°C incubation) the MV-HspA strain efficiently replicated and had a comparable cytopathic effect to MV-GFP on MV producer Vero cells (Figure 3A) and to the other control strains at 37°C incubation (Figure S1). However, at a lower MOI of 0.01 (Figure 3C) MV-HspA showed faster development

of the cytopathic effect as compared to MV-GFP and significantly reduced cell viability to 5% at the final endpoint of the experiment (144-h incubation), versus 20% of the cells surviving following MV-GFP infection at the same time point ($p < 0.05$). As a next step, five tumor cells lines, including breast cancer (MCF-7 and MDA-231 derivative lines), ovarian cancer SR-B2 cells, and sarcoma lines HOS and MG-63 were inoculated with MV strains at different MOIs, and cell viability was analyzed by the MTT method. MV-HspA treatment demonstrated a superior *in vitro* tumor-killing effect as compared to control virus strains against the cancer cell lines tested. Response to MV-HspA treatment of the MV-susceptible human breast cancer MCF-7 cells at an MOI of 0.1 was faster, with more than 70% of the monolayers destroyed by 48-h incubation versus only 38% for the MV-NIS strain (Figure 4A). MV-HspA at later time points (72-h and 120-h infection) killed 85% and 90% of the cells, respectively, versus approximately 50% for the MV-NIS strain ($p < 0.001$). The MV-HspA anti-tumor effect was also superior to MV-GFP ($p < 0.001$) against the MDA-MB-231 derivative breast cancer line, with less than 10% surviving cells at 72 h following infection and almost complete elimination by the end of the experiment at 144-h incubation (Figure 4B). In contrast, more than 25% and 12% of the cells, respectively, were viable after MV-GFP infection at these time points.

The sarcoma HOS cells were very permissive to the MV infection, with an almost 100% cell-killing effect following infection at MOIs of 1.0, 0.5, and 0.1 with both MV-HspA and the control strains. However, MV-HspA showed significantly faster kinetics, with rapid oncolytic effect development within the first 48 h from infection (Figure 4C) and 84% cell killing as compared to only 35% for the MV-NIS strain ($p < 0.001$). The anti-tumor effect against the other MG-63 sarcoma cell line, which exhibits strong interferon (IFN) response upon stimulation (ATCC cell line characteristics), required a higher MOI of 1.0 in order to achieve almost 80% tumor-killing by 72-h infection with MV-HspA. In contrast, 75%–85% of the cells were still viable at later time points following MV-GFP infection (Figure 4D).

MV-HspA Demonstrated a Strong Oncolytic Effect against Ovarian Cancer Cells Both *In Vitro* and *In Vivo*

SR-B2 cells were infected at different MOIs, and cell viability was determined by MTT and trypan blue cell exclusion assays. As shown
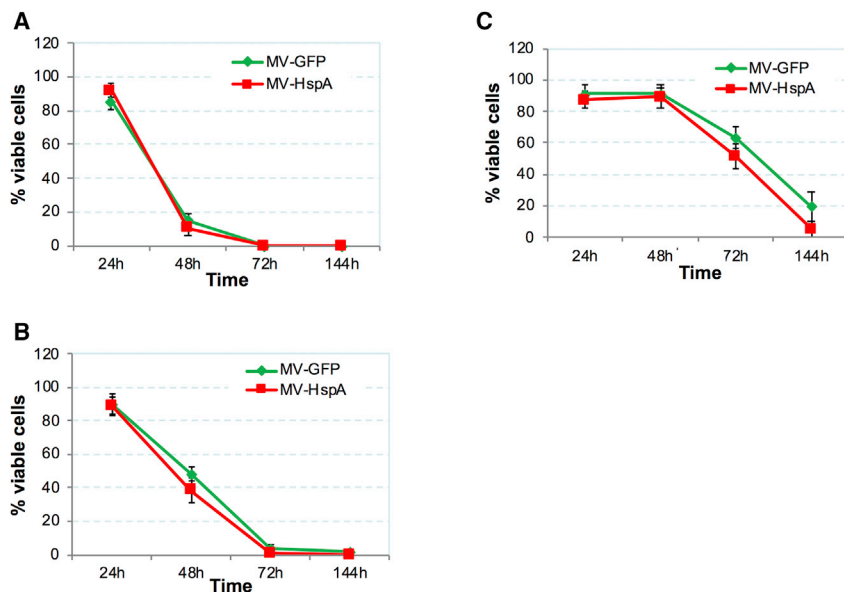
A

C

Figure 3. MV-HspA Infection Kinetics in Vero Cells

(A–C) MTT cell viability assays after infection of the MV producer Vero cell line at an MOI of 1.0 (A), 0.1 (B), and 0.01 (C) of MV-HspA or the MV-GFP control strain. The assays were run and calculated from eight repeats in 96-well plates. At an MOI of 0.01, MV-HspA demonstrated a significant increase in cytopathic effect as compared to MV-GFP following 72- and 144-h infection (p = 0.0064 and p = 0.0029, respectively). Bars indicate standard deviation.

B

by the cell viability assay, a higher MOI of 1.0 MV-GFP killed approximately 80% of the ovarian cancer cells following 96-h-incubation (Figure 5A). However, infection again spread faster in the wells inoculated with HspA-expressing virus, and cell viability was reduced by 80% within first 48 h and reached more than 96% at 96 h versus only 49% and 78% for MV-GFP, respectively (p < 0.001). Similar results were obtained with an MOI of 0.5 (Figure 5B) and when MV-NIS was used as another MV strain (Figure S2). The oncolytic efficacy of MV-HspA was even more prominent at a lower MOI of 0.1, with residual viability of 12%–13% after 72–96 h compared to a much higher viability of 75%–76% following MV-GFP infection (Figure 5C).

The fast replication ability of the recombinant MV-HspA strain was confirmed by immunoblot analysis for accumulation of two of the main MV structural proteins N and P using monoclonal antibodies (mAbs) generated in our laboratory, that is, hybridoma clone 8A11 (IgG1 isotype) against the N protein and 9E11 (IgG2b isotype) against the P protein. Specificity for the corresponding antigen was confirmed by immunoblotting in 293T cells transfected with MV N, P, or V protein-encoding plasmids (Figure S3). Of note, mAb 8A11 has been approved for human use in MV virotherapy clinical trials for detection of MV infection in tumor samples. Western immunoblotting allowed us to characterize the time kinetics of the MV protein synthesis in MV-HspA-infected ovarian cancer cells. Rapid accumulation of N and P proteins was observed within 24–48 h as compared to the MV-GFP (Figure 5D). This correlated with a significant increase of MV-HspA replication and virus mRNA production versus the control MV strain as determined by quantitative RT-PCR (qRT-PCR) for N gene expression (Figure S4). In addition, we evaluated the possible interference of MV-HspA replication with immune response regulation mechanisms in the infected cells. In SR-B2 cells, the MV firefly luciferase (MV-luc) control strain triggered rapid (24-h post-infec-

tion) surface expression of the immune checkpoint PD-L1, which is considered a key tumor immune escape mechanism (Figure 5E). Approximately 10% of the cells were positive with high mean fluorescence intensity (MFI). In contrast, MV-HspA did not induce significant elevation of the PD-L1 expression as compared to the uninfected control cells. PD-L1 was detected in only 0.2% of the infected cells, with significantly lower (<25) relative MFI versus >70 MFI for the MV-luc-infected SR-B2 cells (Figure 5F). Both MV-HspA and MV-luc control virus induced strong release of the immunogenic cell death biomarker HMGB1 in the supernatants at 24 h following infection (Figure 5G). The average secretion by control cells was 18 ng/mL in SR-B2 cells and 23 ng/mL in 293T samples. In SR-B2 cells infected with MV-HspA the effect was stronger (179 ng/mL) but not significant versus MV-luc (153 ng/mL). In 293T cells, MV-HspA infection resulted in a significant 2-fold increase of HMGB1 expression versus MV-luc, that is, 182 ng/mL versus 91 ng/mL, respectively.

MV-HspA-induced IFN response showed delayed kinetics in the post-infection time course. At 24 h post-infection IFN-β expression was detected in MV-GFP-infected cells but not in the supernatants of MV-HspA-infected SR-B2 cells (Figure S5). IFN-β was detected at a higher level than in the control strain at 48-h infection, when the MV-HspA-mediated cytopathic effect with large syncytia formation became prominent and resulted in significant reduction of cell viability. In contrast, IFN-α expression upon MV infection was not detected in SR-B2 cells at these time points (data not shown). These data suggest that despite the rapid accumulation of virus RNA, MV-HspA replication remained undetected by innate immune mechanisms within the first 24 h, which are critical for establishing a productive infection. The qRT-PCR results support this finding and showed a decline of N gene expression in MV-GFP-infected cells by 72 h. In contrast, the number of N gene copies in MV-HspA-infected cells increased more than 400-fold by 72 h of incubation (see Figure S4).

In the ovarian cancer SR-B2 orthotopic xenograft model, mice received two therapeutic doses of 10^6 TCID$_{50}$ of MV strains through the intraperitoneal (i.p.) route of administration. For the control group, which was treated with inactivated virus, the median survival was 27 days (Figure 6). Both MV-HspA and MV-GFP treatment
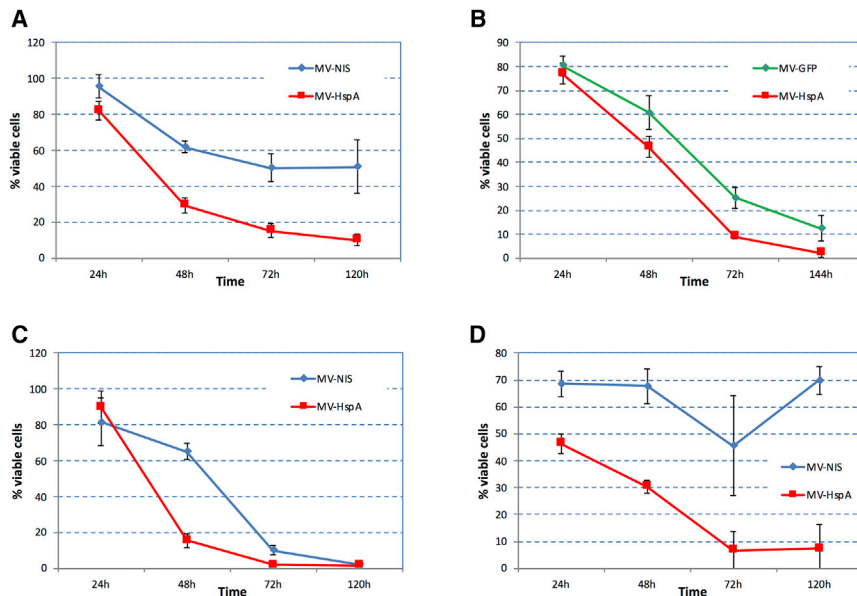
A

B

C

D

Figure 4. MV-HspA Showed a Significant *In Vitro* Anti-tumor Effect against Different Solid Tumor Types

(A and B) The results show MV-HspA infection of the breast cancer MCF-7 line at an MOI of 0.1 (A) and MDA-231-RFP derivative cells at an MOI of 1.0 (B). Each sample was run in 8 separate wells of 96-well plates, and cell viability was determined using an MTT assay. MV-NIS and MV-GFP were used as control strains, respectively. (C and D) MV-HspA oncolytic efficacy was compared to MV-NIS in an MTT assay against two sarcoma cell lines: HOS infected at an MOI of 0.1 (C) and the resistance to MV-NIS-mediated killing MG63 cells following infection at an MOI of 1 (D). Data show mean ±SD at different incubation times.

significantly improved median survival to 64.5 days and 61 days as compared to the control heat-inactivated MV-treated group (p = 0.0027 and p = 0.0037). There was no statistically significant difference between the two treated groups (p > 0.05). These data confirmed that the faster replicating MV-HspA resulted in potent oncolytic *in vivo* activity against an orthotopic ovarian cancer model.

MV-HspA Induced Strong Long-Term Protective Anti-measles Immunity and Antibody Response to *H. pylori* HspA Antigen

The immune response to MV and HspA antigen was analyzed following three repeated immunizations of measles infection-susceptible Ifnarko-CD46Ge transgenic mice. The virus neutralization (VN) test demonstrated a rapid response with development of protective MV neutralizing titers 2 weeks after the first immunization (50% plaque reduction neutralization titer [PRNT$_{50}$] range of 1:106 to 1:1,306). PRNT$_{50}$ titers increased significantly after the second immunization on day 28 and reached highly protective levels corresponding to sterile anti-measles immunity before the third MV-HspA injection on day 42, with an average titer >1:4,400 and no statistical difference between male and female mice (Figures 7A and 7B; Table S1). A durable anti-measles response with protective levels above 1:120 was detected in all mice at the final endpoint of the study (Figure 7C).

An antibody response to purified HspA in an antigen-mediated enzyme-linked immunosorbent assay (ELISA) showed an initial response on day 14 after the first immunization in all except one female of the Ifnarko-CD46Ge mice (Figures 7D and 7E). Anti-HspA antibody titers were boosted in all animals with a range between 1:200 and 1:12,800 after the second and third immunization, suggesting that MV-HspA-infected cells expressed high levels of *H. pylori* HspA antigen *in vivo* and induced strong humoral immunity without any negative interference with the anti-measles vaccine protection.

The humoral response against HspA was long-lasting, with immunized mice having a mean antibody titer 1:3,200 (Figure 7F). This was confirmed by persistence of IgG-secreting memory B cells in the female immunized mice (range, 17–70 spots per 10^6 spleen cells) but not in the male animals in the B cell enzyme-linked immunospot (ELISPOT) assay at the end of the study (Figure S6).

Cell-mediated immunity was evaluated using the ELISPOT assay on isolated spleen cells stimulated with purified HspA or MV-NIS infection at an MOI of 1. All animals maintained strong long-term inflammatory type cell-mediated immunity against MV on the endpoint day 120 of the study as measured by an IFN-γ ELISPOT assay. Spleen cells from non-immunized animals were stimulated in the same way and used as controls (Figure 8). The cellular immune response to MV antigens was detected in all immunized mice, with an average of 656 IFN-γ-positive spots per 10^6 spleen cells. The assay was run following a short overnight MV antigen induction before plating the cells in ELISPOT plates. Following a 72-h induction with 100 ng/mL purified antigen, a cell-mediated response against HspA antigen was detected in five of nine MV-HspA-vaccinated animals (range of 38–166 by IFN-γ-specific spots per 10^6 spleen cells). The Ni-NTA column mock extracts from pET-28a empty vector-transformed *E. coli* BL21 Star (DE3) bacterial cells was used as a control stimulant. Samples were run in duplicates, and results from the control wells were subtracted for calculation of the HspA antigen-specific induction of the IFN-γ response.

DISCUSSION

MV Edmonston vaccine strains have been explored as vaccine and oncolytic live vector for expression of foreign antigens, anti-cancer therapeutic genes, and reporters for monitoring infection spread.[6,27] Insertion of foreign long-length sequences, including multiple genes required for progenitor cell reprograming into the MV genome, is tolerated, and recombinant vectors have been successfully rescued and propagated.[7] We have previously shown that attenuated MV strains represent an excellent vaccine platform for expression of protective antigens of bacterial origin. MV encoding the *H. pylori* NAP
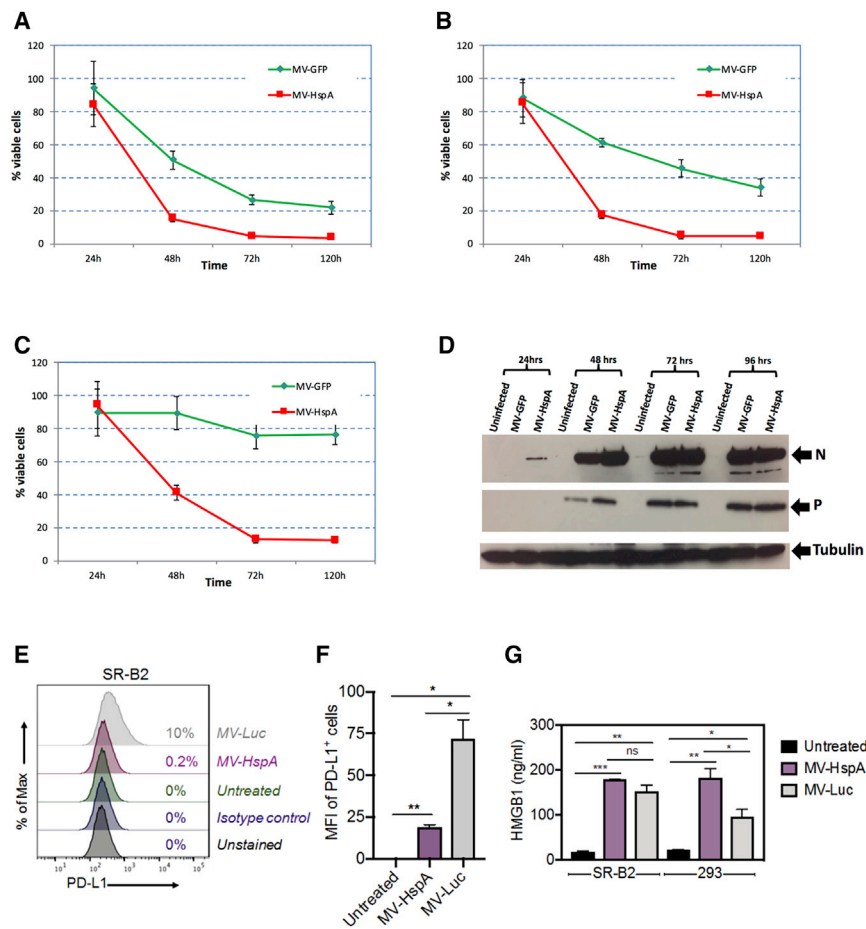
Figure 5. MV-HspA Showed a Strong Anti-tumor Effect against Ovarian Cancer Cells *In Vitro*

(A–C) SR-B2 cells were infected at MOIs of 1.0 (A), 0.5 (B), and 0.1 (C), and cell proliferation was determined at different incubation times using an MTT assay. Each sample was run in 8 separate wells of 96-well plates. Error bars represent the mean ±SD at different incubation times. (D) MV-GFP as used as a control MV strain in the rapid accumulation of the MV N and P proteins reflects MV-HspA faster growth kinetics and a tumor cell-killing effect against SR-B2 cells. For the immunoblot analysis, cells were infected at an MOI of 1.0. N and P expression levels were compared to those of MV-GFP-infected or uninfected control cells. Tubulin-specific antibody was used to confirm equal protein transfer on the PVDF membrane. PD-L1 surface expression by MV-infected SR-B2 cells was analyzed by flow cytometry. (E) The MV-luc control strain-infected cells responded rapidly with approximately 10% positive cells by 24 h versus only 0.2% positive cells following MV-HspA infection. (F) The mean fluorescence intensity (MFI) was also significantly lower in MV-HspA-infected cells as compared to the MV-luc control. (G) The HMGB1 concentration in the supernatants from MV-infected (MOI of 2) SR-B2 and 293T cells was measured by ELISA at 24 h. Data represent the mean of two independent samples, with each sample run in duplicates. Error bars represent standard deviation. Asterisks denote significance: *$p < 0.05$, **$p < 0.01$ and ***$p < 0.001$, respectively.

virulence factor was able to induce robust humoral and cell-mediated immune responses against both NAP and MV.[8] The NAP transgene significantly enhances the oncolytic MV therapeutic efficacy against breast cancer, including a lung metastatic model, which is resistant to virotherapy with conventional oncolytic MV strains.[17] Acting as a potent immunoadjuvant, *H. pylori* NAP boosted significantly the immune response against poor immunogens expressed by the MV vector as chimeric NAP-tagged proteins.[9] These data encouraged additional exploration of the attractive approach of using bacterial virulence factors, infection modulators, and immunostimulatory molecules encoded by replication-competent virus vectors as vaccine candidates and anti-cancer therapeutics.

HspA, a protein with unique function and a key virulence factor, has already been targeted in *H. pylori* vaccine development and demonstrated its efficacy in a multicomponent purified formulation.[23] We cloned the HspA gene in the attenuated MV Edmonston backbone as an additional transcription unit before the N gene and successfully rescued the MV-HspA strain. The polar transcription pattern in negative-strand RNA viruses, such as Paramyxoviridae,[28] creates the opportunity to influence the level of gene expression dependent on the position in the genome of the MV vector.[29] HspA coded up-

stream of the N gene favored the highest degree of expression required for functional intracellular activity and immunogenic potency of the protein. Bacterial heat shock proteins are effective stimulators of a Th1-type cytokine response and are used in dendritic cell-based anti-tumor vaccines.[30–32] Therefore, combining the anti-tumor oncolytic effect of MV Edmonston strain derivatives with immunostimulatory properties of HspA represents a novel combined immunovirotherapy approach. HspA expression boosted significantly MV replication and a faster oncolytic effect *in vitro* against solid tumors of at least three different types, that is, ovarian cancer, breast cancer, and sarcomas. The robust anti-tumor effect against ovarian cancer cells *in vitro* could be explained by the lack of detectable innate immune response to MV-HspA infection at the early stage of infection. Delayed IFN-β release allowed early spread of the virus, and the late IFN-β peak at 48 h could be attributed to the robust cytopathic effect and large syncytia formation.[33] Improved MV replication correlated well with increased viral mRNA production, virus protein synthesis, and rapid accumulation of both released and cell-associated infectious viral particles. Previous reports demonstrated that *H. pylori* infection interferes with heat shock protein signaling, reducing expression of the HSP70, HSP8, and HSF-1 (a transcriptional activator of HSP70) independently of the main *H. pylori* extracellular virulence factor VacA and Cag pathogenicity island.[34] Heat shock proteins are essential stress-induced molecular chaperones that facilitate protein folding and remodeling critical for
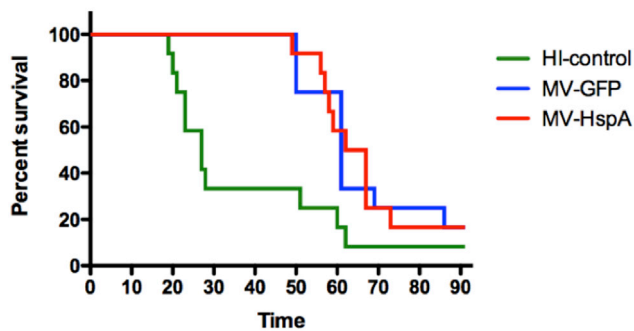
Survival of Data 1:Survival proportions

Figure 6. Animal Survival (Groups of 12 Mice) in the Orthotopic SR-B2 Ovarian Cancer Model
SCID mice were engrafted with SR-B2 cells and treated with two repeated injections of 10^6 TCID$_{50}$ of MV-HspA, MV-GFP, or inactivated MV-GFP. Median survival: heat-inactivated control, 27 days; MV-GFP, 61 days; MV-HspA, 64.5 days. Significance: MV-GFP versus inactivated MV, p = 0.0037; MV-HspA versus inactivated MV, p = 0.0027; MV-GFP versus MV-HspA, not significant (p = 0.907).

virtually all main cellular processes,[35] with evidence of intracellular localization in the cytosol of infected gastric mucosa cells.[36] Proteomic studies showed that *H. pylori* cysteine-rich proteins can interact directly and indirectly in complex formation with human heat shock protein members and other intracellular proteins important in the response to viral and bacterial infection.[37] HspA by itself is a strong promoter of an inflammatory-type cytokine response via the Toll-like receptor-4-mediated signaling pathway.[38,39]

In contrast to the MV-GFP control strain, MV-HspA infection was associated with a delay in the type I IFN response in ovarian cancer cells, which could account for the quick expansion of infection and improved oncolytic effect (see Figure S5). Recently, we identified the IFN-induced protein RSAD2 as a major restriction factor of MV infection and inhibitor of anti-tumor activity against SR-B2 xenografts.[40] Baseline anti-viral state and infection-triggered IFN-stimulated gene expression could predict the response to oncolytic MV therapy,[41] and the differences in eliciting an early IFN response could explain the difference in tumor cell sensitivity to MV-HspA versus control strains. Since the IFN sensitivity is attributed to the P protein gene in the backbone of MV vaccine derivative strains,[42,43] we hypothesized that the HspA transgene could interfere with the IFN response pathway. Our experiments demonstrated that the HspA transgene not only facilitated MV replication but it also regulated the important immune checkpoint axis by inhibiting MV infection-triggered PD-L1 expression in cancer cells (see Figure 7). These data suggest that HspA expressed within MV-HspA-infected cells might retain bacterial chaperonin function, interfering with the cellular protein remodeling machinery by modulating the cellular anti-pathogen immune defense. Crosstalk between IFN type I receptor signaling and the immune checkpoint pathway is known to upregulate autocrine PD-L1 expression.[44] However, the detailed mechanisms involved in the observed HspA transgene immunomod-

ulatory effect on innate immunity and immune response control need to be elucidated in future investigations.

MV infection by itself triggers a pro-inflammatory response that could act synergistically with other therapeutic modalities in cancer treatment.[45] Expression of Th1-type cytokines by MV could significantly enhance immunomodulatory properties of the viral infection and establishment of a stable anti-tumor response.[46] The fast replication and quick release of infectious virus could be the major advantage of MV-HspA as a virotherapeutic agent, and it was supported by *in vivo* data in orthotopic ovarian cancer xenografts. In the ovarian cancer SR-B2 orthotopic xenograft model, MV-HspA demonstrated a strong anti-tumor effect and significantly improved survival of the treated animals. Although the median survival was improved only by 2.5 days as compared to control MV-GFP, the data in nude mouse xenograft models do not fully capture the benefit of MV-HspA treatment, given its immunostimulatory potential. MV-expressing tumor-associated antigens could elicit a cytotoxic lymphocyte response as tumor-specific targeted vaccines.[47] A potential implication of HspA as a therapeutic transgene could be its immunomodulatory impact on the immune checkpoint pathway and pro-immunogenic marker expression by MV-HspA-infected cells. PD-1/PD-L1 immune checkpoint inhibition is one of the main mechanisms of tumor microenvironment alteration and cancer cell escape from immune surveillance. Blockade of the PD-1/PD-L1 interactions is critical for precise T cell-based immunotherapy.[48] The baseline PD-L1 expression and PD-L1 induced in the course of therapy in cancer cells could be a critical impediment for cancer immunotherapy success. Thus, the lack of PD-L1 expression increase in MV-HspA-infected cells could represent a major advantage for clinical translation of virus vectors with improved immune checkpoint surveillance both as oncolytic agents and recombinant vaccines. Generation of antigen-expressing recombinant strains on the MV-HspA backbone would allow combining the favorable effect of PD-1/PD-L1 pathway alteration with the generation of a strong immune response against protein antigens with weak immunogenicity.

Immunization studies with recombinant MV-HspA were performed in the measles-permissive Ifnarko-CD46Ge mouse model. MV susceptible, IFN type I receptor knockout and human CD46 transgenic mice (Ifnarko-CD46Ge) represent a relevant small animal model for studying viral pathogenesis[49] and anti-measles host immune mechanisms.[8,9] Animals responded with development of a protective anti-measles response within 2 weeks after the first immunization dose of MV-HspA. Neutralization titers reached and maintained very high levels of average above 1:4,000 PRNT$_{50}$ at day 120 of the study. Despite that the HspA transgene is accumulating intracellularly and not in a secretory form, an HspA-specific antibody response was detected in all animals following the three-dose immunization course.

Vectored MV vaccines encoding foreign viral antigens, including antigens deriving from viruses associated with emerging virus
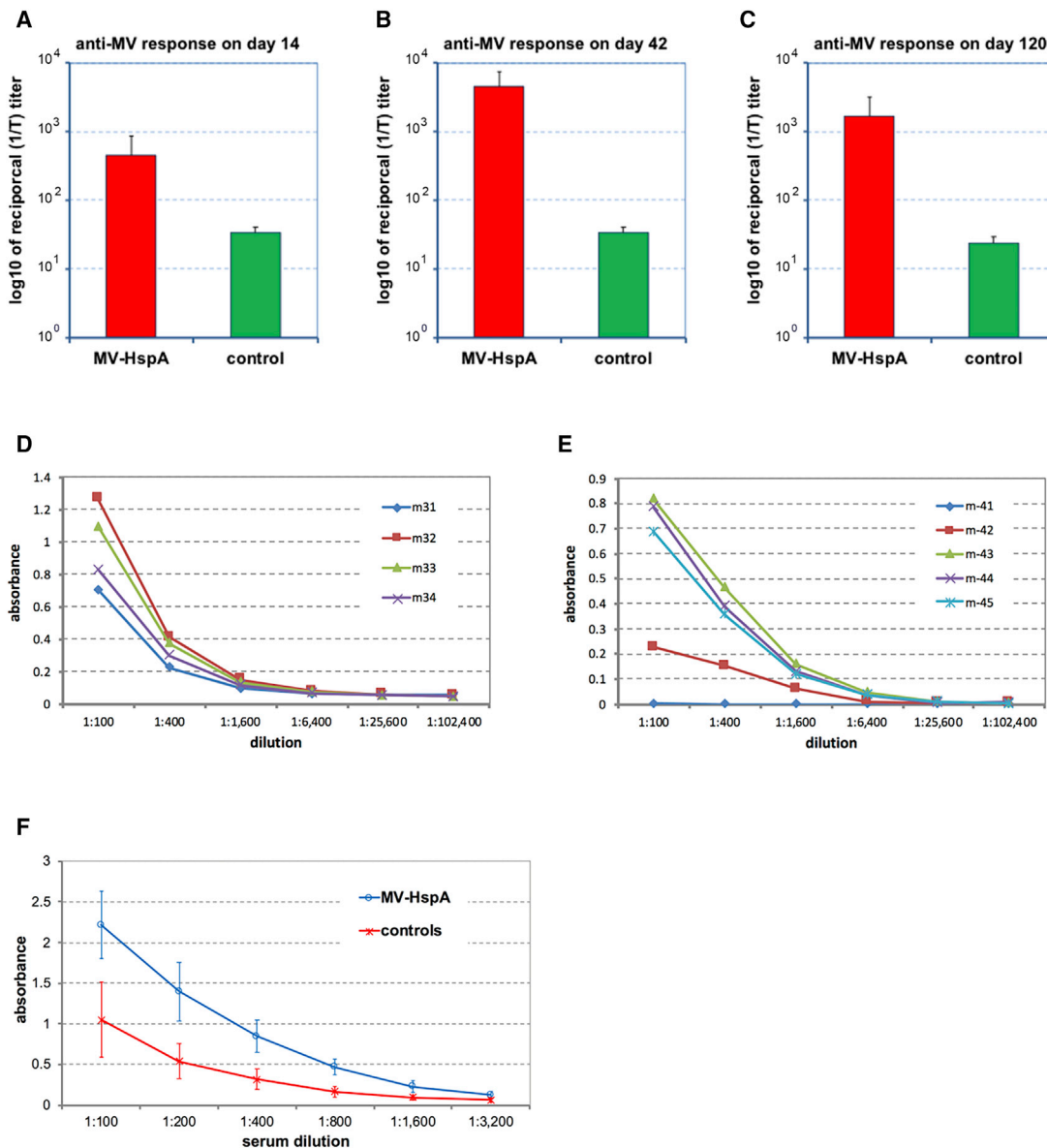
Figure 7. Immune Response against MV-HspA in Measles-Permissive Ifnarko-CD46Ge Transgenic Mice (n = 9)

(A and B) Anti-measles protective virus neutralization titers were detected as early as 14 days after the first immunization with 10^6 TCID$_{50}$ (A) and reached strongly protective PRNT$_{50}$ titers (1:4,435 on average) on day 42 (B) before the third MV-HspA injection. (C) All animals maintained protective anti-measles titers by the end of the study on day 120, with a range from 1:145 to 1:5,078. Control mice (three males, three females) titer range was 1:19-1:52, below the titer considered protective in humans (120 PRNT$_{50}$). The HspA-specific antibody response was determined in antigen-mediated ELISA. (D and E) Anti-HspA antibodies were detected in all male (D) and in all except one of the female mice (E) on day 14 after the first immunization. PET-28 extract-coated wells were used as cutoff controls. (F) On day 120, mice had an average titer of 1:3,200 that was calculated as the highest dilution with absorbance at 450 nm greater than the mean + 2 × SD of the control six non-immune serum samples in the corresponding dilution. Error bars represent the mean ±SD.

infections, demonstrated strong immunogenic potential combined with the excellent safety properties of the attenuated MV strains.[50,51] Models have predicted that the most beneficial strategy for control and eradication of *H. pylori* infection could be immunoprophylaxis at the infant age.[15] Vaccination with dual pathogen targeting based on a live attenuated vector with an already proven safety record could represent a major advantage in this context. Thus, MV-HspA and previously published MV-s-NAP[8] should be explored as a recombinant bivalent vaccine approach inducing both durable anti-measles immunity and targeting protective *H. pylori* antigens with key roles in infection pathogenesis. Previous tests on HspA immunogenicity as a vaccine included recombinant protein expression by insect cells
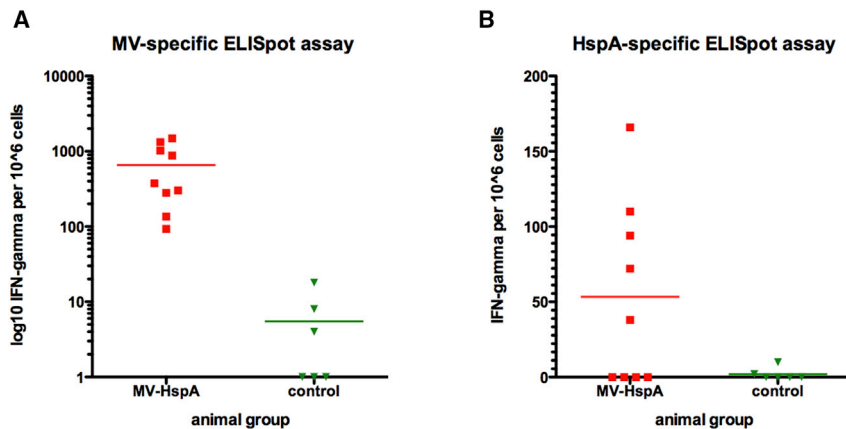
Figure 8. Cell-Mediated Immune Response against HspA and MV Antigens in MV-HspA-immunized Mice

(A and B) IFN-γ ELISPOT assay on isolated spleen cells collected on day 120 and stimulated with MV-NIS (A) at an MOI of 1 or 100 ng/mL of the purified recombinant HspA (B) for 24 or 72 h respectively. Spleen cells stimulated with Ni-NTA mock extracts from pET-28a empty vector-transformed *E. coli* BL21 Star (DE3) bacterial cells were as cutoff controls. Results were compared to spleen cells collected from age-matched control mice (three males, three females) and treated in the same way with the antigens. Samples were run in duplicates, and results from the mock-stimulated control wells were subtracted for the HspA-specific response calculation.

for oral administration.[52] However, to our knowledge the recombinant MV-HspA strain we have constructed represents the first live attenuated virus-based vaccine platform for expression of *H. pylori* or other bacteria derived heat shock protein antigens.

In conclusion, these experiments demonstrate the advantage of genetically engineered MV strains expressing bacterial heat shock proteins and their potential for clinical translation as vaccines and cancer virotherapeutics.

MATERIALS AND METHODS

H. pylori HspA Cloning and Rescue of the MV-HspA Strain

HspA was cloned from genomic DNA of *H. pylori* strain 26695 purchased from the American Type Culture Collection (ATCC, Manassas, VA, USA). HspA was amplified by PCR using primers with MluI and AatII flanking restriction enzyme cloning sites. The PCR product was cloned into the pCRII vector using a TA cloning kit (Thermo Fisher Scientific). A MluI/AatII (New England Biolabs)-digested fragment from the TA vector was isolated and inserted into the full-length MV cDNA plasmid p(+)MV-EGFP, replacing the GFP gene as described previously.[8] The HspA insert into the full-length MV plasmid was verified by DNA sequencing. The recombinant MV-HspA strain was rescued on 293-3-46 cells according to the method established by Radecke et al.[53]

MV Strains, Virus Titration, and Growth Kinetics

MV-HspA and control strains encoding GFP (MV-GFP), sodium iodide symporter (MV-NIS), and firefly luciferase (MV-luc)[54–56] were propagated on Vero cells (ATCC) as described previously.[57] Passages 2 and 3 MV stocks were prepared, and $TCID_{50}$/mL titers were calculated by titration on Vero cells. Titers of the stocks used in the study were in the range of 2.0×10^7 to 6.32×10^7 $TCID_{50}$/mL. A high-grade purified MV-NIS stock was used for the mAb screening and characterization.[9] The one-step MV-HspA growth kinetics was determined by Vero cell inoculation using an MOI of 1.0 and subsequent incubation at 32°C. Cell-associated and supernatant-released viruses were titrated following 24, 48, 72, and 96 h of incubation as described before.[8]

Purification of Recombinant HspA Protein

HspA from *H. pylori* strain 26695 was amplified by PCR and cloned into pET28a bacterial expression plasmid (Novagen) using BamHI and NotI digestion sites. Recombinant HspA was expressed in pET28a vector-transformed *E. coli* BL21 Star (DE3) bacterial cells according to the manufacturer's protocol (Thermo Fisher Scientific).

The 6-His-tagged HspA was purified using a Ni-NTA Fast Start kit (QIAGEN) as described previously.[8] Protein concentration was measured by 280-nm absorbance, and product quality was verified by SDS-PAGE using the Criterion SDS-PAGE system (Bio-Rad). Ni-NTA column extracts from pET28a empty vector-transformed *E. coli* BL21 Star (DE3) cells were used as a control.

Antigen-Mediated ELISA

The 96-well polystyrene plates (Nunc) were coated with 100–300 ng/well of purified HspA antigen in 100 μL of carbonate-bicarbonate buffer (CBB) (pH 9.6). Ni-NTA-eluted preparations extracted from empty vector pET28a-transformed bacteria were used as controls. After overnight incubation at 2°C–8°C the ELISA plates were washed with phosphate-buffered saline (PBS) and blocked for 1 h at room temperature with 1% bovine serum albumin (BSA) in PBS. Mouse sera were serially diluted in PBS with 1% BSA and 0.05% Tween 20 (PBS/T) and added to the plates for a 1-h incubation at room temperature. Following three washings in PBS/T, anti-mouse polyvalent Ig (G, A, M) horseradish peroxidase (HRP) conjugate (Sigma) or rat anti-mouse IgG HRP conjugate (Thermo Fisher Scientific) was used as secondary antibodies in dilutions 1:1,000–1:2,000 for 1 h. Reaction was developed using tetramethylbenzidine (TMB) peroxidase substrate (Bethyl Laboratories). Samples collected from corresponding non-immunized animal groups were used as control sera in the assay.

SDS-PAGE and Immunoblot Assay

Serum-free supernatants and cell lysates were collected from MV-infected cell lines at different MOIs. Purified proteins and cell lysates were mixed 1:1 with sample buffer (under reducing conditions), loaded on 12.5% and 15% Criterion polyacrylamide gels, and resolved using the Criterion electrophoresis system (Bio-Rad). In the

SDS-PAGE analysis, protein bands were visualized by SimplyBlue SafeStain incubation for 2–4 h (Thermo Fisher Scientific).

For immunoblot assays, SDS-PAGE gels were blotted on polyvinylidene (PVDF) membranes (Bio-Rad) using a semi-dry system (Bio-Rad). Membranes were blocked for 1 h in 10% non-fat dry milk (Bio-Rad) in PBS/T and incubated with the primary antibodies or hybridoma supernatant in 10% dry milk in PBS/T. Reaction was incubated for 2 h at room temperature or overnight at 2°C–8°C. Anti-mouse polyvalent Ig (G, A, M) HRP-conjugated antibody (Sigma) and anti-mouse IgG HRP (Santa Cruz Biotechnology) were used as secondary reagents in a 1:2,000 dilution in 10% dry milk in PBS/T. The specific reaction was visualized using a chemiluminescent reagent (Thermo Fisher Scientific).

IFN-γ and B Cell ELISPOT Assay

B and T cell-mediated immunity to HspA and MV antigens was analyzed on isolated spleen lymphocytes of immunized Ifnarko-CD46Ge mice using mouse IFN-γ and IgM/IgG dual-color B cell ELISPOT kits (R&D Systems). Spleen cells were harvested, washed, and plated (5×10^6 cells/well in 1 mL of culture medium) in 24-well plates for stimulation with MV-NIS at an MOI of 0.1, 100 ng/mL purified HspA, and corresponding empty pET-28a control extracts overnight. On the next day 5×10^4 and 5×10^5 cells in 100 μL of medium were transferred to the IFN-γ ELISPOT plates and incubated for 24 or 72 h before the analysis. For the HspA-specific IgM/IgG B cell response detection, spleen cells were transferred to HspA (200 ng/well) or control antigen-coated ELISPOT plates and cultured for 3 days. The reaction was developed following the ELISPOT kit instructions (R&D Systems). Results were analyzed on an ImmunoSpot S4 Pro analyzer (Cellular Technology, Cleveland, OH, USA) using ImmunoSpot version 4.0 software (Cellular Technology).

VN Test

A measles-neutralizing antibody titer was determined using a plaque-reduction microneutralization assay as described previously.[8] Briefly, 2-fold serum dilutions were mixed with 100 $TCID_{50}$ of MV-GFP in 96-well plates in reduced serum Opti-MEM medium (Thermo Fisher Scientific) and incubated for 1 h at 37°C. Vero cells were plated in different 96-well plates at a density of 10^4 per well in 50 μL of Opti-MEM supplemented with 2% FBS. 100 μL of sample mix was added to Vero cells and cultured at 37°C, and the number of GFP-positive syncytia per well was determined following a 48- to 72-h incubation by fluorescent microscopy (Nikon). MV-GFP incubated in Opti-MEM alone was run as control using eight wells in each individual plate. The $PRNT_{50}$ was calculated using the Karber's formula.[58]

In Vitro Cell-Killing Experiments

The cell lines MCF-7, MG-63, and HOS were purchased from ATCC and grown in recommended culture media. Human ovarian cancer SR-B2 cells expressing the red fluorescent protein reporter (RFP) and breast cancer MDA-231-RFP and MDA-231-luc derivative cell lines were described in our previous studies.[59,60] The cell lines were plated in 96- or 12-well plates and infected with the MV strains at different MOIs (0.01–2.0) in Opti-MEM or DMEM with 2% FBS. The infected cells were incubated at 37°C up to 144 h after inoculation. The cell viability was determined at 24, 48, 72, 96, and 144 h using an MTT cell viability kit (ATCC) or trypan blue exclusion assay as described previously.[60,61]

qRT-PCR for N Protein Gene Copies

SR-B2 cells were cultured overnight in 12-well plates and inoculated with MV-HspA or MV-GFP at an MOI of 0.1. Total RNA was isolated at 24-, 48-, and 72-h incubation using an RNeasy kit (QIAGEN). The qRT-PCR for the MV N gene was run using one-step RT-PCR master mix (Thermo Fisher Scientific) and a Roche 480 machine (Roche) as described previously.[62]

Flow Cytometry for PD-L1 Expression

The ovarian cancer SR-B2 cells were infected at an MOI of 2.0 of the MV-HspA or control MV-luc strain in six-well plates. After a 24-h incubation period, cells were harvested, washed in PBS, and resuspended to 10^6 per mL in 2% BSA in PBS. Fluorescein isothiocyanate (FITC)-conjugated antibody specific to human PD-L1 (CD274, clone 28E.2A3) or mouse IgG2b isotype control antibody (both from BioLegend) were added in 1:100 dilution and incubated for 30 min on ice. Then, the cells were washed in PBS and fixed in fixation buffer (BioLegend). The analysis was performed on an LSRFortessa cytometer (BD Biosciences), and results were analyzed using FlowJo software (Tree Star).

ELISA for HMGB1 Expression

The ovarian cancer SR-B2 and 293T cells were infected at an MOI of 2.0 with the MV-HspA or control MV-luc strain in duplicates in six-well plates. Control wells were treated with the corresponding volume of Opti-MEM. Supernatants were collected at 24 h, centrifuged, and stored frozen at −20°C. The HMGB1 released from infected cells was measured following the HMGB1 ELISA kit instructions (IBL International).

ELISA for Human IFN-α and IFN-β Expression

SR-B2 cells were plated in six-well plates and, after the overnight incubation, were infected by adding MV-HspA or MV-GFP at an MOI of 1 to the wells. Supernatants were collected at 24 and 48 h post-infection and stored frozen at −80°C. Type I IFN release by infected cells was analyzed using a human IFN-α ELISA development kit (Mabtech) and human IFN-β Quantikine kit (R&D Systems) according to the recommended protocols. Each sample was run in duplicates, and uninfected cells were used as a control.

In Vivo Experiments

Animal studies were approved by the Mayo Foundation Institutional Animal Care and Use Committee.

Immunization of Mice for Polyclonal HspA-Specific Serum Antibodies

Five- to 6-week-old female BALB/c mice were immunized i.p. with 10 μg of purified HspA dissolved in 100 μL of PBS and mixed 1:1

with complete Freund's adjuvant (Sigma). Immunization was repeated on days 7 and 14 using the antigen mixed with incomplete Freund's adjuvant (Sigma), and 3 weeks later serum was collected and tested for an HspA-specific response in ELISA and immunoblot.

Generation of mAbs against MV Proteins

The mouse myeloma line Sp2/0-Ag14 was purchased from ATCC and grown in the recommended medium. Five-week-old female BALB/c mice were injected with 2×10^6 TCID$_{50}$ of MV-GFP via the i.p. route. Immunization was repeated twice on days 7 and 21, and anti-MV serum antibody titers were determined by ELISA. Mice with the highest titer received a final intravenous (i.v.) boost with 10^6 TCID$_{50}$ MV-GFP. Three days later, spleen cells were harvested and hybridomas were generated by using the Sp2/0-Ag14 hybridoma fusion partner.[63] Hybridomas were grown in DMEM (Sigma) supplemented with 10% FBS and antibiotics (Thermo Fisher Scientific). Hybridoma culture supernatants were tested by antigen-mediated ELISA and immunoblotting for MV antigen-specific mAb production. Hybridomas against MV N and P protein were cloned and culture supernatants were collected. mAbs 8A11 (anti-N) and 9E11 (anti-P) isotypes were identified using an Iso-Strip monoclonal antibody isotyping kit (Santa Cruz Biotechnology) and used for the experiments. Before the hybridoma generation description in the present study, as part of the complete characterization, the N protein-specific mAb 8A11 was tested in immunoblot and immunohistochemistry for detection of MV infection,[40,64] including in formalin-fixed and paraffin-embedded clinical tissue samples.

MV-HspA Immunization of Measles Infection Permissive Mice

Mixed male and female 5- to 6-week old IFN type I receptor knockout mice and human CD46 transgenic Ifnarko-CD46Ge mice (n = 9) were inoculated i.p. with 10^6 TCID$_{50}$ of MV-HspA on days 1, 28, and 42. Mice were bled for serum collection on day 14, prior to the re-immunization on days 28 and 42 and 2 months after the last immunization. Sera from six (three male and three female) non-immunized mice were used as controls. On day 120 of the study, mice were terminally bled and spleen cells were harvested. Spleen cells and serum samples were collected from a second control animal group (n = 6). The measles antibody neutralization titer and HspA-specific antibody response were determined by VN and antigen-mediated ELISA, respectively. Spleen cells were antigen stimulated and used in IFN-γ and IgM/IgG dual-color B cell ELISPOT assays.

MV Treatment in Orthotopic Ovarian Cancer Xenograft Model

Female 5-week-old severe combined immunodeficiency (SCID) mice (12 per group) were engrafted by i.p. injection of 5×10^6 SR-B2 cells in 0.2 mL of PBS. Mice were treated by two i.p. injections on days 7 and 14 with 10^6 TCID$_{50}$ of MV-HspA, MV-GFP, or heat-inactivated MV-GFP control diluted in 0.25 mL of PBS. Mice were monitored daily for development of ascites and weight loss of more than 15%. Survival curves were analyzed according to the Kaplan-Meier method, and median survival times between groups were compared by the log-rank test. A p value of <0.05 was considered as statistically significant.

Statistical Analyses

Statistical analysis was performed using the Microsoft Excel and GraphPad Prism 5.0 analytical software (GraphPad, San Diego, CA, USA).

AUTHOR CONTRIBUTIONS

I.D.I., C.K., and E.G. proposed the study, designed the experiments, and interpreted the results of the MV-HspA work. I.D.I., M.J.F., and E.G. were involved in generation and characterization of the mAbs against MV antigens. I.D.I., C.K., K.V., A.A., and E.P. conducted the experiments. I.D.I. and E.G. wrote the manuscript. All authors have reviewed and approved the manuscript.

CONFLICTS OF INTEREST

E.G. reports grant/research support from MedImmune, Tracon, Genentech, and Bristol-Myers Squibb to the Mayo Clinic; was a consultant for MedImmune with compensation to the Mayo Clinic; and was an Advisory Board member for Karyopharm with compensation to the Mayo Clinic. The remaining authors declare no competing interests.

REFERENCES

1. Griffin, D. (2001). Measles virus. In Field's Virology, D.M. Knipe and P.M. Howley, eds. (Lippincott Williams & Wilkins), pp. 1401–1441.

2. Patel, M.K., Dumolard, L., Nedelec, Y., Sodha, S.V., Steulet, C., Gacic-Dobo, M., Kretsinger, K., McFarland, J., Rota, P.A., and Goodson, J.L. (2019). Progress toward regional measles elimination—worldwide, 2000–2018. MMWR Morb. Mortal. Wkly. Rep. 68, 1105–1111.

3. Robinson, S., and Galanis, E. (2017). Potential and clinical translation of oncolytic measles viruses. Expert Opin. Biol. Ther. 17, 353–363.

4. Msaouel, P., Opyrchal, M., Dispenzieri, A., Peng, K.W., Federspiel, M.J., Russell, S.J., and Galanis, E. (2018). Clinical trials with oncolytic measles virus: current status and future prospects. Curr. Cancer Drug Targets 18, 177–187.

5. Zuniga, A., Wang, Z., Liniger, M., Hangartner, L., Caballero, M., Pavlovic, J., Wild, P., Viret, J.F., Glueck, R., Billeter, M.A., and Naim, H.Y. (2007). Attenuated measles virus as a vaccine vector. Vaccine 25, 2974–2983.

6. Lauer, K.B., Borrow, R., and Blanchard, T.J. (2017). Multivalent and multipathogen viral vector vaccines. Clin. Vaccine Immunol. 24, 1–15.

7. Wang, Q., Vossen, A., Ikeda, Y., and Devaux, P. (2019). Measles vector as a multigene delivery platform facilitating iPSC reprogramming. Gene Ther. 26, 151–164.

8. Iankov, I.D., Haralambieva, I.H., and Galanis, E. (2011). Immunogenicity of attenuated measles virus engineered to express *Helicobacter pylori* neutrophil-activating protein. Vaccine 29, 1710–1720.

9. Iankov, I.D., Federspiel, M.J., and Galanis, E. (2013). Measles virus expressed *Helicobacter pylori* neutrophil-activating protein significantly enhances the immunogenicity of poor immunogens. Vaccine 31, 4795–4801.

10. Cover, T.L., and Blaser, M.J. (2009). *Helicobacter pylori* in health and disease. Gastroenterology 136, 1863–1873.

11. Ferreri, A.J., Ernberg, I., and Copie-Bergman, C. (2009). Infectious agents and lymphoma development: molecular and clinical aspects. J. Intern. Med. 265, 421–438.

12. Kusters, J.G., van Vliet, A.H., and Kuipers, E.J. (2006). Pathogenesis of *Helicobacter pylori* infection. Clin. Microbiol. Rev. 19, 449–490.

13. Frenck, R.W., Jr., and Clemens, J. (2003). Helicobacter in the developing world. Microbes Infect. 5, 705–713.

14. Safavi, M., Sabourian, R., and Foroumadi, A. (2016). Treatment of *Helicobacter pylori* infection: current and future insights. World J. Clin. Cases 4, 5–19.

15. Rupnow, M.F., Chang, A.H., Shachter, R.D., Owens, D.K., and Parsonnet, J. (2009). Cost-effectiveness of a potential prophylactic *Helicobacter pylori* vaccine in the United States. J. Infect. Dis. 200, 1311–1317.

16. de Vries, R., Klok, R.M., Brouwers, J.R., and Postma, M.J. (2009). Cost-effectiveness of a potential future *Helicobacter pylori* vaccine in the Netherlands: the impact of varying the discount rate for health. Vaccine 27, 846–852.

17. Iankov, I.D., Allen, C., Federspiel, M.J., Myers, R.M., Peng, K.W., Ingle, J.N., Russell, S.J., and Galanis, E. (2012). Expression of immunomodulatory neutrophil-activating protein of *Helicobacter pylori* enhances the antitumor activity of oncolytic measles virus. Mol. Ther. 20, 1139–1147.

18. Del Giudice, G., Covacci, A., Telford, J.L., Montecucco, C., and Rappuoli, R. (2001). The design of vaccines against *Helicobacter pylori* and their development. Annu. Rev. Immunol. 19, 523–563.

19. Meza, B., Ascencio, F., Sierra-Beltrán, A.P., Torres, J., and Angulo, C. (2017). A novel design of a multi-antigenic, multistage and multi-epitope vaccine against *Helicobacter pylori*: an in silico approach. Infect. Genet. Evol. 49, 309–317.

20. Cun, S., Li, H., Ge, R., Lin, M.C., and Sun, H. (2008). A histidine-rich and cysteine-rich metal-binding domain at the C terminus of heat shock protein A from *Helicobacter pylori*: implication for nickel homeostasis and bismuth susceptibility. J. Biol. Chem. 283, 15142–15151.

21. Schauer, K., Muller, C., Carrière, M., Labigne, A., Cavazza, C., and De Reuse, H. (2010). The *Helicobacter pylori* GroES cochaperonin HspA functions as a specialized nickel chaperone and sequestration protein through its unique C-terminal extension. J. Bacteriol. 192, 1231–1237.

22. Ge, R., Sun, X., Gu, Q., Watt, R.M., Tanner, J.A., Wong, B.C., Xia, H.H., Huang, J.D., He, Q.Y., and Sun, H. (2007). A proteomic approach for the identification of bismuth-binding proteins in *Helicobacter pylori*. J. Biol. Inorg. Chem. 12, 831–842.

23. Wu, C., Shi, Y., Guo, H., Zou, W.Y., Guo, G., Xie, Q.H., Mao, X.H., Tong, W.D., and Zou, Q.M. (2008). Protection against *Helicobacter pylori* infection in Mongolian gerbil by intragastric or intramuscular administration of *H. pylori* multicomponent vaccine. Helicobacter 13, 191–199.

24. Zhang, X., Zhang, J., Yang, F., Wu, W., Sun, H., Xie, Q., Si, W., Zou, Q., and Yang, Z. (2015). Immunization with heat shock protein A and γ-glutamyl transpeptidase induces reduction on the *Helicobacter pylori* colonization in mice. PLoS ONE 10, e0130391.

25. Wang, L., Liu, X.F., Yun, S., Yuan, X.P., Mao, X.H., Wu, C., Zhang, W.J., Liu, K.Y., Guo, G., Lu, D.S., et al. (2010). Protection against *Helicobacter pylori* infection by a trivalent fusion vaccine based on a fragment of urease B-UreB414. J. Microbiol. 48, 223–228.

26. Kolakofsky, D., Pelet, T., Garcin, D., Hausmann, S., Curran, J., and Roux, L. (1998). Paramyxovirus RNA synthesis and the requirement for hexamer genome length: the rule of six revisited. J. Virol. 72, 891–899.

27. Msaouel, P., Opyrchal, M., Domingo Musibay, E., and Galanis, E. (2013). Oncolytic measles virus strains as novel anticancer agents. Expert Opin. Biol. Ther. 13, 483–502.

28. Lamb, R.A., and Kolakofsky, D. (2001). Paramyxoviridae: the viruses and their replication. In Field's Virology, D.M. Knipe and P.M. Howley, eds. (Lippincott Williams & Wilkins), pp. 1305–1340.

29. Driscoll, C.B., Tonne, J.M., El Khatib, M., Cattaneo, R., Ikeda, Y., and Devaux, P. (2015). Nuclear reprogramming with a non-integrating human RNA virus. Stem Cell Res. Ther. 6, 48.

30. Marcatili, A., Cipollaro de l'Ero, G., Galdiero, M., Folgore, A., and Petrillo, G. (1997). TNF-α, IL-1α, IL-6 and ICAM-1 expression in human keratinocytes stimulated in vitro with *Escherichia coli* heat-shock proteins. Microbiology (Reading) 143, 45–53.

31. Galdiero, M., de l'Ero, G.C., and Marcatili, A. (1997). Cytokine and adhesion molecule expression in human monocytes and endothelial cells stimulated with bacterial heat shock proteins. Infect. Immun. 65, 699–707.

32. Jung, I.D., Shin, S.J., Lee, M.G., Kang, T.H., Han, H.D., Lee, S.J., Kim, W.S., Kim, H.M., Park, W.S., Kim, H.W., et al. (2014). Enhancement of tumor-specific T cell-mediated immunity in dendritic cell-based vaccines by *Mycobacterium tuberculosis* heat shock protein X. J. Immunol. 193, 1233–1245.

33. Herschke, F., Plumet, S., Duhen, T., Azocar, O., Druelle, J., Laine, D., Wild, T.F., Rabourdin-Combe, C., Gerlier, D., and Valentin, H. (2007). Cell-cell fusion induced by measles virus amplifies the type I interferon response. J. Virol. 81, 12859–12871.

34. Axsen, W.S., Styer, C.M., and Solnick, J.V. (2009). Inhibition of heat shock protein expression by *Helicobacter pylori*. Microb. Pathog. 47, 231–236.

35. Genest, O., Wickner, S., and Doyle, S.M. (2019). Hsp90 and Hsp70 chaperones: collaborators in protein remodeling. J. Biol. Chem. 294, 2109–2120.

36. De Luca, A., De Falco, M., Manente, L., Dattilo, D., Lucariello, A., Esposito, V., Gnarini, M., Citro, G., Baldi, A., Tufano, M.A., and Iaquinto, G. (2008). *Helicobacter pylori* heat shock protein B (HspB) localizes in vivo in the gastric mucosa and MALT lymphoma. J. Cell. Physiol. 216, 78–82.

37. Roschitzki, B., Schauer, S., and Mittl, P.R. (2011). Recognition of host proteins by Helicobacter cysteine-rich protein C. Curr. Microbiol. 63, 239–249.

38. Su, Y.L., Yang, J.C., Lee, H., Sheu, F., Hsu, C.H., Lin, S.L., and Chow, L.P. (2015). The C-terminal disulfide bonds of *Helicobacter pylori* GroES are critical for IL-8 secretion via the TLR4-dependent pathway in gastric epithelial cells. J. Immunol. 194, 3997–4007.

39. Lee, H., Su, Y.L., Huang, B.S., Hsieh, F.T., Chang, Y.H., Tzeng, S.R., Hsu, C.H., Huang, P.T., Lou, K.L., Wang, Y.T., and Chow, L.P. (2016). Importance of the C-terminal histidine residues of *Helicobacter pylori* GroES for Toll-like receptor 4 binding and interleukin-8 cytokine production. Sci. Rep. 6, 37367.

40. Kurokawa, C., Iankov, I.D., and Galanis, E. (2019). A key anti-viral protein, RSAD2/VIPERIN, restricts the release of measles virus from infected cells. Virus Res. 2, 145–150.

41. Kurokawa, C., Iankov, I.D., Anderson, S.K., Aderca, I., Leontovich, A.A., Maurer, M.J., Oberg, A.L., Schroeder, M.A., Giannini, C., Greiner, S.M., et al. (2018). Constitutive interferon pathway activation in tumors as an efficacy determinant following oncolytic virotherapy. J. Natl. Cancer Inst. 110, 1123–1132.

42. Haralambieva, I., Iankov, I., Hasegawa, K., Harvey, M., Russell, S.J., and Peng, K.W. (2007). Engineering oncolytic measles virus to circumvent the intracellular innate immune response. Mol. Ther. 15, 588–597.

43. Devaux, P., von Messling, V., Songsungthong, W., Springfeld, C., and Cattaneo, R. (2007). Tyrosine 110 in the measles virus phosphoprotein is required to block STAT1 phosphorylation. Virology 360, 72–83.

44. Xiao, W., Klement, J.D., Lu, C., Ibrahim, M.L., and Liu, K. (2018). IFNAR1 controls autocrine type I IFN regulation of PD-L1 expression in myeloid-derived suppressor cells. J. Immunol. 201, 264–277.

45. Rajaraman, S., Canjuga, D., Ghosh, M., Codrea, M.C., Sieger, R., Wedekink, F., Tatagiba, M., Koch, M., Lauer, U.M., Nahnsen, S., et al. (2018). Measles virus-based treatments trigger a pro-inflammatory cascade and a distinctive immunopeptidome in glioblastoma. Mol. Ther. Oncolytics 12, 147–161.

46. Veinalde, R., Grossardt, C., Hartmann, L., Bourgeois-Daigneault, M.C., Bell, J.C., Jäger, D., von Kalle, C., Ungerechts, G., and Engeland, C.E. (2017). Oncolytic measles virus encoding interleukin-12 mediates potent antitumor effects through T cell activation. OncoImmunology 6, e1285992.

47. Hutzler, S., Erbar, S., Jabulowsky, R.A., Hanauer, J.R.H., Schnotz, J.H., Beissert, T., Bodmer, B.S., Eberle, R., Boller, K., Klamp, T., et al. (2017). Antigen-specific oncolytic MV-based tumor vaccines through presentation of selected tumor-associated antigens on infected cells or virus-like particles. Sci. Rep. 7, 16892.

48. Havel, J.J., Chowell, D., and Chan, T.A. (2019). The evolving landscape of biomarkers for checkpoint inhibitor immunotherapy. Nat. Rev. Cancer 19, 133–150.

49. Mrkic, B., Pavlovic, J., Rülicke, T., Volpe, P., Buchholz, C.J., Hourcade, D., Atkinson, J.P., Aguzzi, A., and Cattaneo, R. (1998). Measles virus spread and pathogenesis in genetically modified mice. J. Virol. 72, 7420–7427.

50. Nürnberger, C., Bodmer, B.S., Fiedler, A.H., Gabriel, G., and Mühlebach, M.D. (2019). A measles virus-based vaccine candidate mediates protection against Zika Virus in an allogeneic mouse pregnancy model. J. Virol. 93, e01485–e01518.

51. Gerke, C., Frantz, P.N., Ramsauer, K., and Tangy, F. (2019). Measles-vectored vaccine approaches against viral infections: a focus on Chikungunya. Expert Rev. Vaccines 18, 393–403.

52. Zhang, X., Shen, W., Lu, Y., Zheng, X., Xue, R., Cao, G., Pan, Z., and Gong, C. (2011). Expression of UreB and HspA of Helicobacter pylori in silkworm pupae and identification of its immunogenicity. Mol. Biol. Rep. 38, 3173–3180.

53. Radecke, F., Spielhofer, P., Schneider, H., Kaelin, K., Huber, M., Dötsch, C., Christiansen, G., and Billeter, M.A. (1995). Rescue of measles viruses from cloned DNA. EMBO J. 14, 5773–5784.

54. Duprex, W.P., McQuaid, S., Hangartner, L., Billeter, M.A., and Rima, B.K. (1999). Observation of measles virus cell-to-cell spread in astrocytoma cells by using a green fluorescent protein-expressing recombinant virus. J. Virol. 73, 9568–9575.

55. Dingli, D., Peng, K.W., Harvey, M.E., Greipp, P.R., O'Connor, M.K., Cattaneo, R., Morris, J.C., and Russell, S.J. (2004). Image-guided radiovirotherapy for multiple myeloma using a recombinant measles virus expressing the thyroidal sodium iodide symporter. Blood 103, 1641–1646.

56. Msaouel, P., Iankov, I.D., Allen, C., Morris, J.C., von Messling, V., Cattaneo, R., Koutsilieris, M., Russell, S.J., and Galanis, E. (2009). Engineered measles virus as a novel oncolytic therapy against prostate cancer. Prostate 69, 82–91.

57. Iankov, I.D., Hillestad, M.L., Dietz, A.B., Russell, S.J., and Galanis, E. (2009). Converting tumor-specific markers into reporters of oncolytic virus infection. Mol. Ther. 17, 1395–1403.

58. Haralambieva, I.H., Ovsyannikova, I.G., Vierkant, R.A., and Poland, G.A. (2008). Development of a novel efficient fluorescence-based plaque reduction microneutralization assay for measles virus immunity. Clin. Vaccine Immunol. 15, 1054–1059.

59. Iankov, I.D., Blechacz, B., Liu, C., Schmeckpeper, J.D., Tarara, J.E., Federspiel, M.J., Caplice, N., and Russell, S.J. (2007). Infected cell carriers: a new strategy for systemic delivery of oncolytic measles viruses in cancer virotherapy. Mol. Ther. 15, 114–122.

60. Iankov, I.D., Msaouel, P., Allen, C., Federspiel, M.J., Bulur, P.A., Dietz, A.B., Gastineau, D., Ikeda, Y., Ingle, J.N., Russell, S.J., and Galanis, E. (2010). Demonstration of anti-tumor activity of oncolytic measles virus strains in a malignant pleural effusion breast cancer model. Breast Cancer Res. Treat. 122, 745–754.

61. Opyrchal, M., Allen, C., Msaouel, P., Iankov, I., and Galanis, E. (2013). Inhibition of Rho-associated coiled-coil-forming kinase increases efficacy of measles virotherapy. Cancer Gene Ther. 20, 630–637.

62. Galanis, E., Atherton, P.J., Maurer, M.J., Knutson, K.L., Dowdy, S.C., Cliby, W.A., Haluska, P., Jr., Long, H.J., Oberg, A., Aderca, I., et al. (2015). Oncolytic measles virus expressing the sodium iodide symporter to treat drug-resistant ovarian cancer. Cancer Res. 75, 22–30.

63. Campbell, A.M. (1991). Monoclonal antibody and immunosensor technology. In Laboratory Techniques in Biochemistry and Molecular Biology, Volume 23 (Elsevier), pp. 189–204.

64. Domingo-Musibay, E., Allen, C., Kurokawa, C., Hardcastle, J.J., Aderca, I., Msaouel, P., Bansal, A., Jiang, H., DeGrado, T.R., and Galanis, E. (2014). Measles Edmonston vaccine strain derivatives have potent oncolytic activity against osteosarcoma. Cancer Gene Ther. 21, 483–490.